ICCES, vol.4, no.3, pp.137-143, 2007

Non-thermal Statistical Mechanics of Disordered Structures and Materials

A.H.W. Ngan[1]

Summary

When a random structure is loaded by far-field stresses, the elements inside will not be subject to the same forces because of structural inhomogeneities. Such a system represents an interesting analog to a thermal system at equilibrium – the structural irregularities qualify for a description by a Shannon-like entropy, and there is also the usual (e.g. elastic) strain energy. When an entropy is related to energy, one immediately steps into the familiar field of statistical mechanics, but for a strained random structure, the real (Kelvin) temperature plays no role. Instead, an effective temperature exists but this is not the Kelvin temperature. The proper statistical mechanics framework that should be used to describe such systems is therefore non-thermal.

Using low-density elastic networks as prototype systems, this paper reviews recent computer simulation and experimental results that support such a non-thermal statistical mechanics framework. These results show the existence of an effective temperature in the description of these structures. As a second example, the dynamic formation of dislocation patterns during plastic deformation or annealing of crystals is also discussed within the same statistical mechanics framework.

keywords: statistical mechanics; random materials; dislocation patterning

Introduction

Either by design or otherwise, many engineering materials are randomly structured. Examples include grain piles, polymeric scaffold materials for tissue engineering applications, metallic foams and so on. Because of structural randomness, the internal force distribution in these materials due to external loadings would not be uniform, yet a thorough understanding of the force distribution is of paramount importance in the development of, for example, yield criteria for these materials.

Most previous investigations on random materials focused on mean-field behaviors involving regular, periodic structures [1]. Although a mean-field understanding is essential for elastic behavior, failure of these materials depends on extreme internal forces. Post-yield phenomena such as local buckling and shear bands are well-known to occur [2], but the onset of these phenomena is determined by the first failure of those elements sustaining the largest *elastic* forces. An understanding of the *variance* of the internal elastic forces is therefore of paramount importance in understanding the first-failure conditions of these structures. However, structural

---

[1] Department of Mechanical Engineering, The University of Hong Kong, Pokfulam Road, Hong Kong, P.R. China

irregularities have only been explicitly considered by a few groups of authors [3-6]. The simulated structures in these studies were different from case to case and so a universal picture is not yet available. Another approach is to add an empirical, volume-dependent term in an assumed constitutive law to reflect the high plastic compressibility of the material [1], but this "black-box" approach avoids directly treating structural randomness.

A completely different view of the subject was provided by Edwards [7] who advocated the use of a statistical entropy to describe the states of random structures. The present author took the additional step to relate Edwards' entropy to the strain energy in these systems to complete an analog with thermodynamics [8-9]. In the following, the theory and the key computer simulation and experimental results are reviewed.

The Non-thermal Free Energy

The basic assumption of the present author's theory is that a non-thermal system attains mechanical equilibrium or steady state when an analog of the free energy

$$F = U - \theta S, \tag{1}$$

reaches a local minimum, i.e. $\delta F = 0$, at a constant θ. Here U is the strain energy and S the macroscopic configurational entropy, in the sense defined by Edwards [7], and because the problem is non-thermal, θ is simply a linking factor and not the Kelvin temperature. The condition $\delta F = 0$ is simply a statement that the strain energy U is minimized at constant S, and since θ behaves as a Lagrange multiplier for the constraint on S, it is a measure of the constant value of S. Thus, the condition $\delta F = 0$ means the finding of a metastable equilibrium state; the system cannot reach the global equilibrium state (at $\theta = 0$) in general because of certain "frustrations" present. In the following, the condition $\delta F = 0$ will be applied to predict mechanical equilibrium of static structures as well as the steady state of a dynamic system.

Elastic Networks

As a prototype example, we look at a loaded structure made up of joining struts together (fig. 1). Each strut in the network will sustain an axial force f, a shear force s, and a bending moment m. Simple beam analysis shows that the strain energy of a given strut is $W \approx C_f f^2 + C_s s^2 + C_m m^2$, where the C's are material and dimensional constants [9]. For an entire network, or an ensemble of similar replicas of such a network, the forces and moments will follow distributions $P_i(i)$ where $i = f$, s or m, and so the strain energy functional U is

$$U = C_f \int f^2 P_f(f)\, df \; + \; C_s \int s^2 P_s(s)\, ds \; + \; C_m \int m^2 P_m(m)\, dm. \tag{2}$$

Under the assumption of an ergodic force/moment-space, the entropy functional is given by

$$S = -k_f \int P_f(f) \ln[P_f(f)]\, df - k_s \int P_s(s) \ln[P_s(s)]\, ds - k_m \int P_m(m) \ln[P_m(m)]\, dm\,, \tag{3}$$

where k_f, k_s and k_m are Boltzmann-like constants. The conditions $\delta F/\delta P_i = 0$ ($i = f$, s or m) give rise to Gaussian forms of the probability density functions

$$P_i(i) = A\ \exp[-\kappa(i - i_o)^2], \tag{4}$$

where $\kappa = C_i/k_i\theta$, and A and i_o are normalization constants.

The ergodicity assumption can be loosely understood by the observation that in a disordered system, the force network is very random [10] and so there is no *a priori* biasing in the force-space. The best way to justify ergodicity, however, is to see if the prediction agrees with experiment. Fig. 1 shows an experiment in which the axial forces f were measured from 2-D silicone networks [11]. The measured axial forces indeed follow a Gaussian distribution as predicted by eqn. (4).

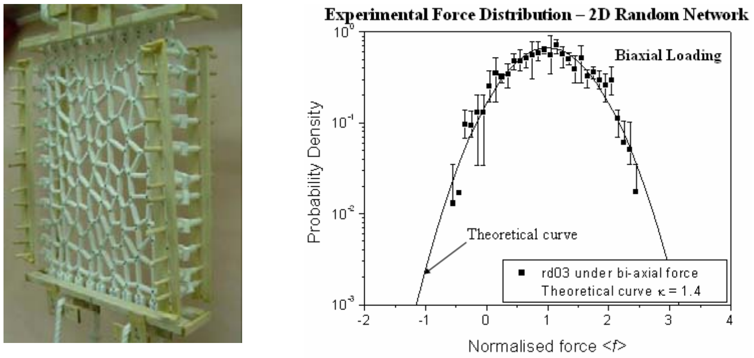

Figure 1: Experimental measurement of axial force distribution in 2-D elastic networks. The left panel shows the experimental setup [11]. The network is made of silicone and the axial forces in the members inside were measured from the displacements of the nodes upon load application.

The above experiment only allowed probability density change of about 2 orders of magnitude to be measurable. To sample even rarer forces, finite element simulations were carried out. 2-D and 3-D elastic networks were simulated using the FEAP finite element package developed by R.L. Taylor. Fig. 2 shows portions of a simulated perturbed square grid (2-D) and a cubic grid (3-D). A series of increasingly irregular structures were built from a regular square or cubic grid by randomly displacing each node in the grid within a range which is a certain fraction r_d (< 0.5) of the mean grid spacing. The fraction r_d then becomes a parameter characterising the randomness of the structure. The simulated grids typically consisted of 10,000 to 20,000 struts. The linear elastic behaviour of the structures under different load states was calculated using the Euler-Beam Element in the FEAP package. Fig. 3(a) shows the simulated axial force distribution in 2-D grids with different values of r_d under hydrostatic loading. It can be seen that the sharpness of the axial force distribution decreases as r_d, or the structural randomness, increases. Fig. 3(b) shows the axial force distributions under biaxial pure shear. At $r_d = 0$, the distribution comprises two delta functions positioned at two (bifurcated) values of the mean force. This is to be expected because in the regular square grid configuration ($r_d = 0$), all struts which are aligned parallel to the tensile axis will be subject to the same tensile force, and all those parallel to the compression axis will be subject to the same compressive force. As r_d increases from zero, the structure becomes increasingly perturbed and the force distribution becomes more spread as shown in fig. 3(b). The model curves in fig. 3 are all Gaussian curves and they fit the simulated data very well. The parameter κ shown there is an inverse measure of the effective temperature θ, and it can be seen that as structural randomness increases, the effective temperature increases. Results in 3-D show similar features.

For load mixities other than the hydrostatic or pure shear states, the force distributions can be obtained by superposition of the hydrostatic and pure shear states. As an example, a uniaxial tensile load state with load σ can be obtained by superposition of a hydrostatic state of stress $\sigma/2$ and a pure-shear state with principal stresses $\pm\sigma/2$. Denoting the force distribution under the hydrostatic and the pure-shear load state respectively $P_i^h(i)$ and $P_i^d(i)$, the distribution under the superimposing load state is,

$$P_i(i) = \int_{-\infty}^{\infty} P_i^h(i-t)\, P_i^d(t)\, dt. \tag{5}$$

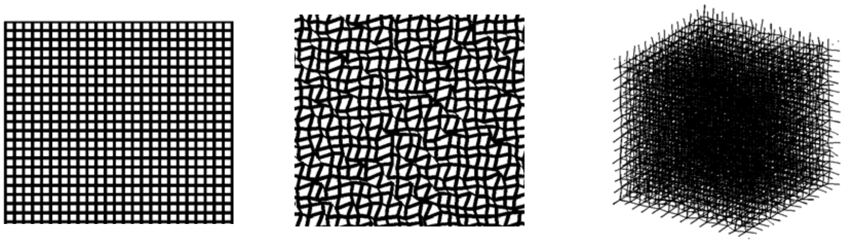

Figure 2: 2-D and 3-D grids used in finite element simulation. First grid has $r_d = 0$. The last two grids have $r_d = 0.4$.

Fig. 4 shows the predicted axial force distribution (the solid curve) in a 2-D grid under uniaxial loading, which is the convolution of two Gaussian functions centred at 0.5 and 1.5 of the abscissa. There is no fitting parameter involved in the predicted

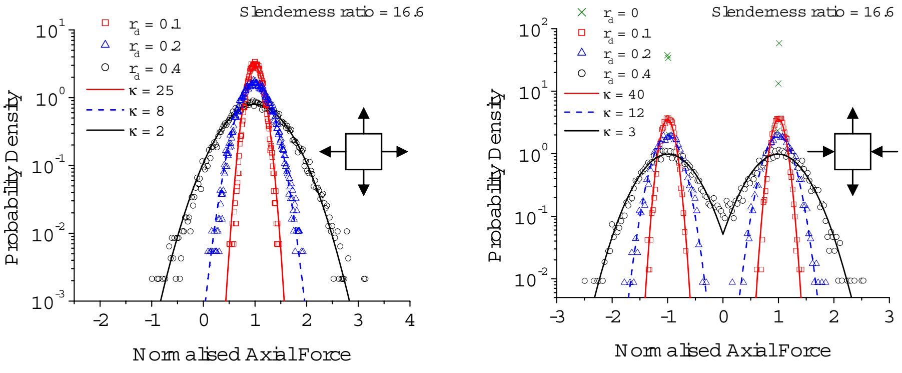

(a) (b)

Figure 3: Axial force distributions in 2-D grids calculated using finite element simulation under (a) hydrostatic loading and (b) biaxial pure shear loading.

force distribution here and the agreement with the finite element results (the discrete points) is excellent. With the force distributions at different load mixities worked out this way, the failure criteria for the structure can be constructed using a survival probability concept [9]. Fig. 5 shows the predicted first-yield and buckling loci (the triangles and squares respectively), in comparison with a plastic collapse mean-field theory [12] (the circles).

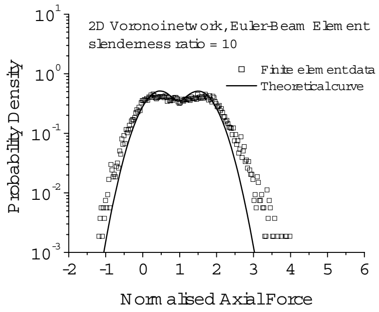

Figure 4: Axial force distributions of 2-D perturbed square grid under unaxial loading.

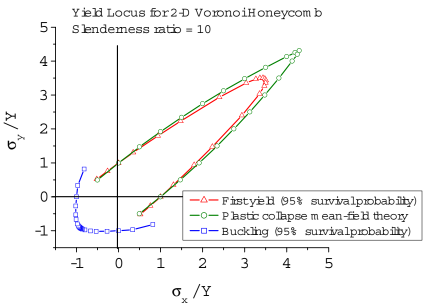

Figure 5: Predicted yield locus of 2-D perturbed square grid. Y is material yield strength.

Dislocation Patterning

As an example to illustrate the condition $\delta F = 0$ in an evolving system, let us turn to the formation of dislocation patterns during plastic deformation or annealing of crystals. Hähner proposed that dislocation patterning is driven by noise [13], but this view is challenged by recent dislocation dynamics simulations by Thomson [14], who showed that dislocation patterning is a consequence of a balance between

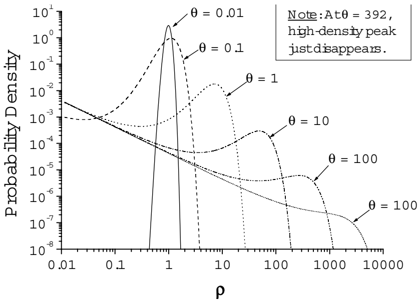

Figure 6: Predicted steady-state dislocation density distribution [15].

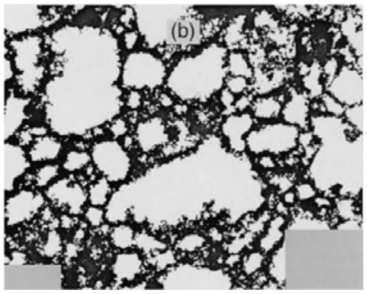

Figure 7: Experimental fractal pattern of dislocations [16].

energetics and noise. The mutual interaction energy between dislocations drives the system towards ordering, but as the system evolves, frustrations to ordering arise due to the noisy back stresses in the slip planes. This is in the same spirit of the condition $\delta F = 0$ in this work, which implies $\delta U = \theta\,\delta S$ at equilibrium or steady state. The present author exploited the condition $\delta U = \theta\,\delta S$ in an analytical manner [15]. Anticipating that the long range interactions between dislocations are difficult to deal with analytically, he used simple relations to express the energy distribution, ε, on the lattice sites of the system in terms of the local dislocation density, ρ. This amounts to the adoption of a field method for the problem, instead of one based on multi-particles. For low dislocation densities, the following energy function was used,

$$\varepsilon(\rho) = \frac{\alpha\mu b^2}{4}\ln\left(\frac{\rho}{\rho_{\min}}\right), \tag{6}$$

where the pre-logarithmic factor is a constant and ρ_{min} refers to the outer cut-off radius for the dislocation distribution. Note that this energy function represents dislocation repulsion, and for attraction, another function was used [15]. The strain energy and entropy were then given by $U = \int \varepsilon P(\varepsilon)d\varepsilon$ and $S = -k\int P(\varepsilon)\ln[P(\varepsilon)]d\varepsilon$, and the condition $\delta F/\delta P = 0$ gives rise to the following steady-state distribution of the dislocation density

$$P(\rho) = \frac{A}{\rho}\exp\left[\frac{\rho}{\theta}\,(c - \ln\rho)\right], \tag{7}$$

where A and c are normalization constants. Fig. 6 plots eqn. (7) at different chosen values of θ . At small values of θ (e.g. 0.01), $P(\rho)$ is uni-modal and corresponds to a state of homogeneous spatial distribution of dislocations. At higher values of θ (e.g. 10), $P(\rho)$ is twin-peaked at a low density and a high-density, corresponding to cell formation. At even higher values of θ (e.g. 1000), $P(\rho)$ is a power law, corresponding to a fractal geometry of patterning, a real example of which is shown in fig. 7.

Conclusions

A general statistical mechanics principle for describing static or dynamic equilibrium of non-thermal systems is proposed. Application of this principle to elastic random networks yields predictions that are in good agreement with experimental and finite element simulated results. The dynamic problem of dislocation patterning also seems to be describable by this principle.

References

1. MF Ashby, AG Evans, NA Fleck *et al.*, *Metal Foams – A Design Guide*, (Butterworth-Heinemann: Boston, 2000).
2. H Bart-Smit, A-F Bastawros, DR Mumm *et al.*, *Acta Mater.* 46, 3583 (1998).
3. DW Overaker, AM Cuitino, NA Langrana, *J. App. Mech. Trans. ASME*, 65, 748 (1998).
4. C Chen, TJ Lu, NA Fleck, *J. Mech. Phys. Solids*, 47, 2235 (1999).
5. HS Kim, STS Al-Hassani, *Int. J. Mech. Sci.*, 43, 2453 (2001).
6. CH Chuang, JS Huang, *Acta Mech.*, 159, 157 (2002).
7. SF Edwards, in *Granular Matter – An Interdisciplinary Approach*, ed. A. Mehta, (Springer-Verlag: New York, 1994), Chp. 4, p. 121.
8. AHW Ngan, *Phys. Rev. E*, 68, 011301 (2003).
9. AHW Ngan, 2005(a), *Proc. Roy. Soc. London A*, 461, 433 (2005); *ibid*, 461, 1423 (2005).
10. CH Liu, SR Nagel, DA Schecter *et al.*, *Science*, 269, 513 (1995).
11. SH Chan, AHW Ngan, to appear in *Mech. Mater.*
12. LJ Gibson, MF Ashby, *Cellular Solids – Structure and Properties*, (Pergamon Press: Oxford, 1988), p. 103.
13. P Hähner, *Appl. Phys.* A, 62, 473 (1996).
14. R Thomson, M Koslowski, R LeSar, *Phys. Rev.* B, 73, 024104 (2006).
15. AHW Ngan, *Scripta Mater.*, 52, 1005 (2005).
16. M Zaiser, K Bay, P Hähner, *Acta Mater.*, 47, 2463 (1998).